Elaboration of host $P2X_7R$-P_{38}MAPK axis involvement against intracellular leishmania donovani by Spergulin-A: a comprehensive study

Niladri Mukherjee [a¥], Saswati Banerjee [a¥], Sk. Abdul Amin[b], Tarun Jha[b], Sriparna Datta[c], Krishna Das Saha[a*]

[a]Cancer Biology and Inflammatory Disorder Division, CSIR-Indian Institute of Chemical Biology, 4 Raja S. C. Mullick Road, Kolkata-700032, India

[b]Natural Science Laboratory, Department of Pharmaceutical Technology, Division of Medicinal & Pharmaceutical Chemistry, P. O. Box 17020, Jadavpur University, Kolkata, India.

[c]Department of Chemical Technology, University of Calcutta, Kolkata 700009, India

Email address: krishna@iicb.res.in (Krishna Das Saha); [¥] Equal contribution, *Corresponding Author

Current drugs are inadequate for the treatment of visceral leishmaniasis an immunosuppressive ailment caused by *Leishmania donovani*. Regrettably, there is no plant-origin antileishmanial drug present. $P2X_7R$ is constitutively present on macrophage surfaces and can be a putative therapeutic target in intra-macrophage pathogens with function attributes towards inflammation, host cell apoptosis, altered redox and phagolysosomal maturation by activating p_{38}MAPK. Here we demonstrated that the initial interaction of Spergulin-A, a triterpenoid saponin with macrophages was mediated through $P2X_7R$ involving the signaling cascade intermediates Ca^{++}, P_{38}MAPK, and NF-κβ. P_{38}MAPK involvement shown to have specific and stern importance in leishmanial killing with increased NF-κBp65. Phago-lysosomal maturation by Spergulin-A also campaigns for another contribution of $P2X_7R$. In vivo evaluation of the anti-leishmanial activity of Spergulin-A was monitored through $P2X_7R$, P_{38}MAPK, and NF-κβ in murine spleen and bone-marrow macrophages and advocated Spergulin-A of being a natural compound of leishmanicidal functions which acted through the $P2X_7R$-P_{38}MAPK axis.

The obligate intra-macrophage parasite *Leishmania donovani* causes the sternest form of leishmaniasis (visceral) and if left untreated can reach casualty as high as 100% within 2 years of infection in developing countries.[1] VL is widespread in tropical and temperate areas and is endemic in 100 countries with an approximate yearly occurrence of 500,000 cases, of which 70,000 people expire every year.[2] Miltefosine, Sodium antimony gluconate, Pentamidine, and Amphotericin B are applied as the choice of chemotherapeutics, however, reported occasions of toxicity or resistance.[3] *Leishmania* parasites have developed various successful strategies for the manipulation of parental activities of macrophage-like antigen presentation, nitric oxide intermediates, and oxygen radical generation and cytokine production.[4] Despite elaborate literature on leishmanial host-pathogen interaction, there is scope for an explicit revelation of compound mediated distortion of intracellular signaling cascades that can subvert parasite propagation and multiplication and can advise new therapeutic stratagems.

Botanicals or phytochemicals have proven their worth as potent therapeutics and are applied as medication against different and various types of human and animal ailments. However, unluckily VL remains an exception even after serious efforts from different groups of scientists and drug companies.[5] Reports of potent plant-derived anti-leishmanial agents are there in the literature,[6] however, mostly performed against the vector-borne promastigote form of the parasite.[7] Our previous effort demonstrated that triterpenoid saponin, Spergulin-A, isolated from a perennial shrub *Glinus oppositifolius* is a potent intracellular antileishmanial compound besides being an immune-modulator.[5] Scientific documentation in this particular area of interest also publicized that triterpenoid saponin of *Careya arborea* and some water-insoluble saponin acted as potent leishmanicidal agents.[8-10]

$P2X_7R$ (a purinergic receptor) is constitutively present on macrophage surfaces with function attributes towards inflammation, apoptosis and intracellular pathogen control.[11] Modulation of macrophage biology in respect to $P2X_7R$ expression alteration is monitored in

Leishmania amazonensis and other intracellular pathogens like *Toxoplasma*, *Brucella* *Cryptosporidium* and *Microsporidia*.[12-16] $P2X_7R$ over-expression can be a putative chemotherapeutic strategy in intra-macrophage pathogens. $P2X_7R$ expression is positively correlated with inflammation, host cell apoptosis, generation of ROS and NO as well as phagolysosomal maturation;[11] all are different strategies for intra-macrophage pathogen killing and absence or underexpression of the $P2X_7R$ have been found with underachieved intracellular pathogen control.[11] Existing literature suggests that activation of $P2X_7R$ can trigger mitogen-activated protein kinases (MAPKs), including P_{38}MAPKs.[17]

Activation of p_{38}MAPK in respect to the $P2X_7R$ over-expression leads to the generation of ROS and NO through NADPH oxidase is also mentioned in the literature[18,19] and embrace consequence in intra-MΦ pathogen control strategies which also comprises leishmanial parasites. Regulation of iNOS expression in macrophages is managed by MAPK signaling molecules with closely associated with NF- κB activation.[20] It was reported that P_{38}MAPK can phosphorylate Rab5 an important step in the endosome maturation process and critical in intracellular leishmanial killing[21] and our previous finding denoted that P_{38}MAPK phosphorylation was decisively responsible for maturation of phagolysosomal complexes and subsequent leishmanicidal activity.[2] Importance of MAPKs in establishment and maintenance of their infection also favoured by the fact that viscerotropic *L. donovani* parasites alleviate MAPK phosphorylation and thus cut of the MAPK signaling cascades towards possible leishmanicidal outcome in naive murine bone marrow-derived macrophages[22] with NF-kB being the prime transcription factor in NO production[23] with evidence that P_{38}MAPK activation is crucial in *L. donovani* infection abolition.[24] Phagosome-lysosome fusion is also an important innate-effector immune response of host macrophages the process of which is maintained by sequential acquisition and removal of different proteins of hydrolases and peptidases in nature and aided in degrading intracellular pathogens which includes leishmanial parasites.[25] The

phagolysosome fusion is also critically acquainted by enhanced $P2X_7R$ expression and managed through bivalent calcium ion efflux and RhoA-Phospholipase D controlled pathway.[11]

Screening compounds toward purinergic receptor modifications have identified structurally diversified compounds over two thousand and almost one-third of them are being natural products having an affinity towards these receptors. As for example teniposide, a semi-synthetic podophyllotoxin derivative can inhibit $P2X_7R$, whereas, agelasine and garcinolic acid,[26] potentially activate the same. In recent years efforts are made towards the identification of compounds that can modulate P2X receptors aiming towards novel chemotherapeutic measurements towards diseases associated with inflammation.[27,28] Extracts of the traditional Chinese medicinal plant, *Panax ginseng* can also activate $P2X_7$ [29] which further identified ginsenosides, triterpenoid saponins found in the root extract of plants for $P2X_7R$ activation properties.[30] Conversely, the *R. longifolia* extract and fractions found to have an inhibitory effect on the $P2X_7R$ leading to their anti-inflammatory function.[31] Additionally, there are ample reports of triterpenoid saponins interacting with different groups of MAPKs including P_{38}MAPK in conferring their cytotoxic or protective roles.[32]

To explore the molecular insights in depicting the intracellular leishmanicidal function of the triterpenoid saponin Spergulin-A, we have emphasized on the involvement of $P2X_7R$ and downstream pathways involved. We checked the *in silico* binding affinity of Spergulin-A with $P2X_7R$. $P2X_7R$ blockage having a hindrance towards the reduction of Spergulin-A mediated leishmanial killing strongly advocates for its association and significance. Involvement of P_{38}MAPK shown to have specific and stern importance in leishmanial killing as with increased NF-κBp65 mediated ROS and NO production reciprocal with parasite reduction and this phenomenon also secondarily established by simultaneous expression analysis of P_{38}MAPK and Gp91-phox, NADPH oxidase family member. Phago-lysosomal maturation promotion in mediating intracellular leishmanial killing by Spergulin-A also

campaigns for another contribution of $P2X_7R$ as well as multipotent effectiveness of Spergulin-A of being a natural product supposed to act like. Finally, the in vitro observation was clarified in vivo for Spergulin-A of being a natural compound of leishmanicidal functions and acted through the $P2X_7R$- P_{38}MAPK axis.

Results

Involvement of the $P2X_7$ receptor in mediating intracellular anti-leishmanial activity of Spergulin-A. At the commencement of the evaluation of antileishmanial affectivity of Spergulin-A against RAW 264.7 MΦ internalized parasites, increasing doses of Spergulin-A (Fig. 1a) was applied for 24 h. Spergulin-A was found to be efficient against the intercellular parasites in a dose-dependent manner; however above 30µg/mL of doses, the antileishmanial activity reached a plateau. Therefore, we have selected the dose of 30µg/mL for a detailed assessment of the intracellular anti-leishmanial activity of Spergulin-A. In our previous report, we had also elaborated that this dose is also perfectly safe against the host RAW 264.7 MΦs and that Spergulin-A was not effective against the acellular promastigote or intermediate axenic amastigote forms of *L. Donovani* at diverse dose applied dose range.[5]

Use of Brilliant Blue G (BB-G) as a selective $P2X_7R$ antagonist[33] was adequate in literature against both in vivo[34] and in vitro systems[35]. Different IC50 values for different cell lines had been reported in the literature and also against a related mouse macrophage cell line (J774.G8) with applied dose range well within 10 µM,[35,36] however not conclusive against RAW 264.7 MΦs. We evaluated the dose range for RAW 264.7 MΦ survival in accordance with the view of the dose range application for its inhibitory purposes against $P2X_7R$ (Fig. 1b). The dose 10µM of BB-G was selected as $P2X_7R$ antagonist in this study to be applied in vitro against RAW 264.7 MΦs as about 92% of the exposed cells were alive after 24 h (Fig. 1b) and the dose is well within the accepted $P2X_7R$ antagonist range in literature.

Thereafter, the contribution of $P2X_7R$ in intracellular *L. donovani* infection and Spergulin-A mediated leishmanicidal function was thoroughly examined (Fig. 1c, d, e). Co-expression of CFSE-tagged *L. donovani* and subsequent $P2X_7R$ expression was monitored by FACS during infection and Spergulin-A (30µg/mL) treatment, with or without BB-G, the $P2X_7R$ antagonist (Fig. 1c i-vi). $P2X_7R$ expression was highest in the treated panel with expected lowest CFSE-tagged *L. Donovani* existence and application of BB-G in treatment panel lowered both the $P2X_7R$ expression and *L. Donovani* removal. Spergulin-A treatment exhibited a significant rise of $P2X_7R$ expressing MΦs of about 44.3% of the parent population in connection with intracellular parasite removal. Whereas, all other panels $P2X_7R$ expressing MΦs were about or below 5% of the parent population with or without BB-G application (Fig. 1c i-vi). And it was also noticed that $P2X_7R$ antagonist BB-G application significantly lowered Spergulin-A mediated intracellular *L. Donovani* removal (Fig. 1c iv-vi) and thus avow important role of $P2X_7R$ in Spergulin-A activated the intracellular leishmanicidal function.

The dose-dependent implication of Spergulin-A in intracellular leishmanial removal and subsequent aversion by BB-G application which resulted in $P2X_7R$ blockage was monitored (Fig. 1d). In all the applied Spergulin-A doses, it was observed that BB-G application lowered the leishmanicidal property of Spergulin-A significantly. Confocal micrographs of CFSE-tagged intracellular *L. donovani* with subsequent $P2X_7R$ expression were monitored for Spergulin-A treatment as well as BB-G application (Fig. 1e). It was obvious from the micrographs that Spergulin-A treatment was able to increase $P2X_7R$ expression and intracellular *L. Donovani* removal whereas the application of the $P2X_7R$ antagonist resulted in profuse existence of the parasite despite the Spergulin-A treatment (Fig. 1e).

This experimental evidences suggested that Spergulin-A mediated its intracellular leishmanicidal action with close assistance with $P2X_7R$ and subsequent signaling pathways linked with over-expression of $P2X_7R$. Therefore, downstream signaling intermediates

associated with $P2X_7R$ should be closely monitored for accessing the precise involvement of $P2X_7R$ in Spergulin-A mediated leishmanial killing.

Spergulin-A treatment has effects on the $P2X_7$ receptor-dependent intracellular Ca^{++} release. It is documented that $P2X_7R$ activation can lead to Ca^{++} influx and resulted in mycobacterial removal.[37] This Ca^{++} influx is definitely of great consequence in case of intracellular leishmanial killing as this increased Ca^{++} titer is linked with phagolysosomal fusion, P_{38}MAPK activation and increased release of NO and ROS along with the altered release of pro and anti-inflammatory cytokines; all of them have leishmanicidal function actively or passively. Thus it is important to monitor the Ca^{++} influx during Spergulin-A treatment and also link the event with $P2X_7R$ activation. A set of FACS analyses with $P2X_7R$ and Ca^{++} corresponding to Fura2M was expressed both graphically and through histograms of fluorescence index and percentage of cells expressing the $P2X_7R$ and Ca^{++} for normal, *L. donovani* parasitized, different doses of Spergulin-A treated MΦs both BB-G exposed and un-exposed (Fig. 2a-c). Mean fluorescence index equivalent of the expressions of both $P2X_7R$ and Ca^{++} was significantly higher in Spergulin-A treated panels and that too in a dose-dependent manner compared to either normal or infected MΦs, and with the application of BB-G, both these expressions got lowered compared to the corresponding BB-G unexposed panels (Fig. 2b). Subsequently, the percentage of $P2X_7R$ and Ca^{++} expressing cells against the parent population also higher for the treated panels and the application of $P2X_7R$ agonist BB-G not only lowered the $P2X_7R$ expressing population but also have diminishing the effect on Ca^{++} expressing cells (Fig. 2c). These results strongly advocated the involvement and dependence between $P2X_7R$ expression and Ca^{++} influx in Spergulin-A mediated anti-leishmanial function.

P_{38}MAPK expression alteration affects Spergulin-A mediated anti-leishmanial activity with $P2X_7$ receptor involvement. The involvement of P_{38}MAPK was evaluated in *L. donovani* infection headway and also the effect of Spergulin-A with the involvement of

P_{38}MAPK towards infection riddance as analyzed by flow cytometry (Fig. 3a). Apart from the panels where P_{38}MAPK inhibitor (SB203580) was used (Fig. 3a iv-vi) almost all the cells were expressing P_{38}MAPK either infected or treated with Spergulin-A (Fig. 3a i-iii). The difference lies in the expression level of P_{38}MAPK. Compared to the control MΦ panel, infection with *L. donovani* comprehensively reduced P_{38}MAPK (Fig. 3a ii and vii). However, Spergulin-A treatment increased the P_{38}MAPK intensity (Fig. 3a iii and vii) and thus possibly has a very precise correlation with the reduced intracellular parasitic count as when SB203580 was used parasitic count also decreased along with the P_{38}MAPK expression (Fig. 3a v-vii).

Co-expression analyses of $P2X_7R$ and P_{38}MAPK were evaluated by confocal microscopy (Fig. 3b). For the control MΦs, both the expressions of $P2X_7R$ and P_{38}MAPK were at a basal level and for the infected and infected with BB-G their expression were down-regulated more precisely P_{38}MAPK expression. Whereas, in the Spergulin-A treated panel both $P2X_7R$ and P_{38}MAPK were visually overexpressed several folds (Fig. 3b) in accordance with the anti-leishmanial effect demonstrated previously. However, the application of BB-G, the $P2X_7R$ antagonist lowered the expression of P_{38}MAPK. Inhibitor mediated underexpression of P_{38}MAPK in the treated panels demonstrated compromised intracellular parasite removal (Fig. 3a) and confocal micrographs (Fig. 3b) suggested that $P2X_7R$ activation can positively regulate P_{38}MAPK expression and most importantly both of them are essential in intracellular Spergulin-A mediated the anti-leishmanial effect of which P_{38}MAPK act downstream of $P2X_7R$.

NF-κBp65 expression alteration in Spergulin-A mediated leishmanicidal activity. Likewise, the connection of NF-κB in Spergulin-A mediated infection control was also monitored (Fig. 3c). The trend was almost alike of P_{38}MAPK expression, parasitic infection down-regulated the expression altitude of NF-κB and Spergulin-A treatment was noticed to up-regulate their expression when applied in the infection panel and in this case also the inhibitor

(Curcumin) were noticed to down-regulate NF-κB expressions with moderate increase of the parasitic load even when co-applied with Spergulin-A (Fig. 3c vi, vii).

ROS and NO participate in anti-leishmanial effects of Spergulin-A. Changes in the production of ROS as well as NO in respect to *L. donovani* infection and Spergulin-A treatment was measured by flow cytometry (Fig. 4a, b) and confocal micrographs (Fig. 4c) with the aid of fluorescent dyes DCFDA and DAF-2 DA respectively. It was observed that ROS production was downregulated with respect to *L. donovani* infection and got up-regulated in MΦs with Spergulin-A (30 μg/mL). In comparison to infected MΦs, Spergulin-A (30 μg/mL) exposure elevated ROS production in the infected MΦs (Fig. 4a iv, vi) which is in the alignment of the lessened parasite load in them (Fig. 4c). However, when NAC has applied the ROS abrogation (Fig. 4a v, vi) also leads to substantial loss of the parasiticidal activity of Spergulin-A (Fig. 4c).

Spergulin-A (30 μg/ml) treatment was found to encourage the NO production in the infected MΦs (Fig. 4b v, vii). It was found that the NO production has a positive effect in checking the parasite load inside the MΦs as NMMA application in the Spergulin-A treated infected MΦs reduced the effectivity of the compound (Fig. 4b vi, Fig. 4c) and strongly support the anti-parasitic activity is regulated by NO.

Expression alteration of p-P_{38}MAPK, p-NF-κBp65, and Gp91-phox in intervening ROS and NO involvement of Spergulin-A mediated anti-leishmanial effect. Gp91-phox the glycosylated subunit of the heterodimer phagocytic NADPH oxidase flavocytochrome b558, plays a crucial role in regulating the redox status of MΦs and thus can serve as a marker of the alteration of oxidative stress due to Spergulin-A treatment in the infected MΦs, aimed towards an explanation of the parasitic burden alteration treated with it at different doses. Spergulin-A at different doses (10, 20 and 30μg/mL) applied in the infected MΦs and levels of Gp91-phox was evaluated for both p-P_{38}MAPK and NF-κBp65 (Rel A) positive MΦs as

evaluated by both FACS (Fig. 5a) and confocal microscopy (Fig. 5b) (for only p-P_{38}MAPK). Gp91-phox expression was simultaneously up-regulated with increasing doses of Spergulin-A along with the increment of p-P_{38}MAPK expression (Fig. 5a i-v (upper panels) and Fig. 5a vi). Likewise, Gp91-phox expression was also found to be elevated with respect to NF-κBp65 expression along with Spergulin-A in a dose-dependent manner (Fig. 5a i-v (lower panels) and Fig. 5a vii).

Confocal images provided substantial evidence that with the increasing doses Spergulin-A boosted p-P_{38}MAPK expression and also Gp91-phox expression simultaneously (Fig. 5b). Infection with *L. donovani* lowered both p-P_{38}MAPK and Gp91-phox expression in them compared to the control (Fig. 7b).

Phago-lysosomal maturation promotion by Spergulin-A in respect to its anti-leishmanial activity. Phagolysosomal maturation considered a significant process to chuck out the intracellular pathogens of phagocytic cells and the pathogens promoted multiple ways to evade this sequential process. Spergulin-A mediated dynamics of Rab 5 an early phagosomal marker and CathepsinD, a late phagosomal marker was observed by confocal microscopy (Fig. 6a). *L. donovani* infection was found to suppress these markers compared to the control MΦs. Whereas, the dose-dependent application of Spergulin-A found to amplified both Rab5 and CathepsinD expression and signified the occurrence of phagolysosomal fusion and demonstrated a key role of this event during leishmanicidal property arbitrated by Spergulin-A (Fig. 6a).

In Vivo Evaluation of anti-leishmanial activity of Spergulin-A in lights of P_{38}-MAPK and $P2X_7$ receptor involvement. Evaluation of the intracellular anti-leishmanial activity of Spergulin-A in vitro against RAW 264.7 MΦs strongly favored the involvement of $P2X_7R$ activation and subsequent participation of P_{38}MAPK and NF-κBp65 downstream. Therefore an in vivo evaluation of the anti-leishmanial activity of Spergulin-A with a demonstration of the

expression alteration analyses of the aforementioned key mediators could have positively linked ours in vitro observations with its leishmanicidal affectivity in vivo. After treatment schedule (Control and Treated group received 30mg/kg b.wt. of Spergulin-A for every alternate day for 10 doses) was over mice were sacrificed and spleen and bone marrow MΦs were harvested for each group and evaluated by flow cytometry for the linked expressions of $P2X_7R$-$P_{38}MAPK$ and $P2X_7R$-NF-κBp65 against spleen MΦs (Fig. 6b) and for $P2X_7R$-$P_{38}MAPK$ against bone marrow MΦs (Fig. 6c).

From the observations made against spleen MΦs the mean fluorescence index values for $P2X_7R$ against both the experiments showed that the treated panels showed highest $P2X_7R$ activation and which was found to be least for the infected panels (Fig. 6b vii, viii) and subsequent expressions of $P_{38}MAPK$ (Fig. 6b vii) and NF-κBp65 (Fig. 6b vii) showed the same pattern; highest for the treated panels. However, for the Bone marrow MΦs although $P2X_7R$ expression was highest in the treated panel (Fig. 6c iii, iv), $P_{38}MAPK$ expression in the treated panel was less than the infected panel (Fig. 6c ii, iv) which slightly differs from our all previous observations both in vitro and in vivo combined.

The in vivo findings confirmed the in vitro findings and were perfectly in accordance of the pathway of action speculated from the in vitro findings combined for the intracellular activity evaluation of Spergulin-A; precisely with the involvement of $P2X_7R$, Ca^{++} influx, $P_{38}MAPK$, NF-κBp65, ROS, NO and phagolysosomal maturation being the key mediators sequentially. A graphical presentation of the step-wise anti-leishmanial activity propagation by Spergulin-A has been demonstrated in Fig. 7d.

In silico binding assessment of Spergulin A with $P2X_7$ Receptor. The possible binding mode of Spergulin A with its putative target $P2X_7$ was analyed by *in silico* methods. Molecular docking study was employed to check the binding mode of investigated compound i.e., Spergulin A toward target $P2X_7$ (PDB: 5U1X). The molecular docking result illustrates few

hydrogen bonding interactions between the Spergulin A and $P2X_7$ receptor as shown in Fig. 7a. The docked conformation of Spergulin A with $P2X_7$ indicates that the sulfonyl function interact with Gln116, Trp167 (Fig. 7b). The amino acid residue Arg295 is found to form another hydrogen bonding interaction with the oxygen atom of pyran nucleus (Fig. 7c). Moreover, it is also noticed that the non-sugar part of Spergulin A is exposed to solvent accessable surface area of the receptor.

Discussion

Leishmaniasis is a poorly investigated disease mainly affecting people in countries that are developing and with challenged health practices. *Leishmania* living within the harsh environment of phagocytes has developed strategies for prompt physiological adaptation, escape from first-line defense systems and ability to inhibit a number of host cell functions.[38] To endure and blossom inside macrophages *Leishmania* adopt various strategies to modulate its physiology and signal kinetics. The direct influence of the parasite to the macrophages linked to the suppressed generation of nitric oxide and oxidative burst and also their inhibitory biological.[39,40] Indirectly, *Leishmania* influences the antigen presentation and T cell tasks in a way that macrophage deactivation guides towards parasite endurance mainly by amendment of host cell signaling of different kinases and phosphatases.[41] Being the host cell for the parasite, any modulation of the macrophages also has an effect on the immune system and thus helping their survival by overall immunomodulation of the host. Our previous effort[5] demonstrated that *G. oppositifolius* and an isolated triterpenoid saponin, Spergulin-A was inconsistent of direct leishmanicidal effect of against promastigotes and axenic amastigotes however proved to be a potent intracellular antileishmanial mediator besides being an immune-modulator measured in vitro in RAW 264.7 MΦs those infected with an *L. donovani* virulent strain. This observation opens for the scope for precise demonstration of the pathways involved in its intracellular anti-

leishmanial effect and involvement and possible activation of $P2X_7R$ has been considered. $P2X_7R$ reported being constitutively expressed on MΦ surfaces and also reported to be associated with signaling cascades of inflammation, apoptosis and subsequent intracellular pathogen control.[11] Additively, intracellular anti-leishmanial attributes of Spergulin-A demonstrating the involvement of the purinergic receptor $P2X_7$ also hypothesized on the reports of compounds screened towards the purinergic receptor amendments that about one-third of the structurally diversified compounds are being natural products with a proven affinity towards these purinergic receptors.[42]

Reduction of Spergulin-A mediated intra-MΦ leishmanial count was found to be linked with $P2X_7R$ activation and this reduction was hindered with $P2X_7R$ antagonist BB-G application and thus confirmed $P2X_7R$ involvement and importance (Fig. 1a-e). Existing literature suggested that $P2X_7R$ possibly contributes to the removal of intracellular parasites namely *Chlamydia*, *Leishmania*, *Toxoplasma*,[43,44] and *Mycobacterium tuberculosis* by mediating strong pro-inflammatory and cytotoxic activity.[45] $P2X_7R$ receptor activation was found to be helpful in reducing *L. amazonensis* parasitic load in macrophages via leukotriene B4 (LTB4) production.[46] Interestingly enough, $P2X_7$ knock out mice were observed to possess increased lesion size and the parasitic load of *L. amazonensis* with an unwarranted $CD4^+$ T cell proliferation.[47]

$P2X_7R$ activation with extracellular stimuli like ATP can initiate opening of cation-specific ion channel and result in the influx of Ca^{++} and the efflux of K^+ and with extended exposure able to create pores in the plasma membrane resulted in the passage of larger molecules.[11] Our experimental verification confirmed Spergulin-A activated $P2X_7R$ mediated Ca^{++} influx (Fig. 2) and unleashed a key mediator in intracellular leishmanial control.

Changes in the concentration of intracellular Ca^{2+} and PI3K activity are essential for proper phagosomal maturation.[48] Ca^{++} is a key second messenger and cytosolic build-up of

Ca^{++} can lead to synaptic transmission, macrophage activation and apoptosis.[49] More interestingly, the cytosolic Ca^{++} concentration affects the phagosomal maturation process by modulating membrane fusion between phagosomes and lysosomal vesicles by activating phospholipase D via RhoA, which can ultimately perish intracellular pathogens like *Leishmania*[50] this phagolysosomal fusion can also mediated by regulating the activities of two Ca^{2+}-dependent effector proteins, calmodulin and the multifunctional serine/threonine-protein kinase CaMKII.[51] Spergulin-A mediated phagolysosomal maturation was confirmed in the treated parasitized MΦs (Fig. 6a) by examining co-expression of early Rab5 and late CathepsinD phagolysosomal markers in the treated cells and provided confirmation of the event in intracellular parasite control.

An influx of Ca^{++} can activate the P_{38}MAPK, which in turn stimulates a number of downstream effector signaling cascades.[52] The connection of phosphorylated P_{38}MAPK and leishmanial removal was closely monitored with Spergulin-A treatment (Fig. 3a, b). With infection p-P_{38}MAPK level lowered and treatment with Spergulin-A resulted in elevated p-P_{38}MAPK and diminished intracellular parasite count which again reversed with P_{38}MAPK inhibitor application and thus one can conclude from the results the close association of P_{38}MAPK activation and leishmanial control. The same observation pattern was elaborated for NF-κBp65 (Fig. 3c) wherewith the application of inhibitor compromised Spergulin-A mediated intracellular parasite control with associated NF-κBp65 down-expression. Existing reports also suggested that impaired P_{38}MAPK expression during host-parasite interaction at the primary hours proven beneficial during subsequent *L. donovani* infection establishment[24] also P_{38}MAPK inactivation by *Leishmania* parasites can lead to the iNOS inhibition and inferior NO production.[39] Host invasion by intra-macrophage pathogens is frequently associated with the restraining of NF-κBp65 total levels in infected macrophages, and this reduction, in turn, can modulate the gene expressions necessary during the normal

immunological clearance of the parasites from the host cells.[53] Phosphorylated P_{38}MAPK also promotes the association of NADPH oxidase at the cell membrane and resulted in production and release of superoxide (O_2^-),[54] enhanced NF-κBp65 activation lead to the ensuing transcription of inducible nitric oxide synthase (iNOS) and production of nitric oxide (NO),[55] as well as production of tumour necrosis factor (TNF) and IL-6.[2] Spergulin-A was monitored to activate Gp91-phox, a glycosylated subunit of NADPH oxidase flavocytochrome b558 and also a marker of the NOX activity[56] with subsequent upregulated p-P_{38}MAPK and p-NF-κBp65 expression (Fig. 5).

Enhanced production of ROS after $P2X_7R$ activation is well recognized in MΦs,[57] mediated by NOX2 additionally also augment mitochondrial ROS.[58] *Leishmania* parasites inside macrophages acclimatize various intimidating conditions during blood transmission, and ROS and RNS by host macrophages.[59] At the onset of leishmanial infection, superoxide production resulted from the oxidative burst due to phagocytosis[60] and later NO is produced after activation of macrophages by IFN-y and TNF [61] resulting in abolition of intracellular parasites.[62] The active subversion of ROS and NO production due to leishmanial infection was noticed to be minimized during Spergulin-A treatment and application of their abrogators minimized the anti-leishmanial effect of the compound (Fig. 4) and thus signifies the importance of ROS and NO in intracellular parasite removal.

Meanwhile, a molecular docking study was performed to get a primary idea about the binding interaction between Spergulin A and its putative target $P2X_7$. Few hydrozen bonding interactions are observed between Spergulin A and amino acids at allosteric site binding of $P2X_7$ (PDB: 5U1X). The docked conformation of Spergulin A with $P2X_7$ indicates the non-sugar part of Spergulin A is exposed to solvent accessable surface area.

Finally, in vitro results from activity evaluation of Spergulin-A mediated intracellular anti-leishmanial effect was directed to the inference that $P2X_7R$-P_{38}MAPK activation is the

key mediator of the said action with the downstream involvement of Ca^{++} regulated ROS, NO and phagolysosomal fusion as the effecter cascade. A flow diagram of which was depicted in Fig. 7d. Additionally, in vivo evaluation in determining the effect of Spergulin-A also established the fact that $P2X_7R$ and $P_{38}MAPK$ expression was evidently upregulated (Fig. 7a-c) and confirmed the in vitro findings.

Methods

Materials. Cell culture medium, Roswell Park Memorial Institute-1640 (RPMI-1640) and M-199, fetal bovine serum (FBS), penicillin-streptomycin (PS), and HEPES were acquired from Gibco BRL, Grand Island, NY, USA. Tissue culture plastic wares were acquired from NUNC (Roskilde, Denmark) and DAPI (4′,6-diamidino-2-phenylindole dihydrochloride), Lysotracker Red, CFSE and FURA 2-AM from Invitrogen, CA. Primary antibodies, secondary antibodies, and inhibitors were obtained from Santa Cruz Biotechnology, Santa Cruz, CA and Cell signaling technologies, USA.

Macrophages. Murine macrophage (MΦ) cell line RAW 264.7 (American Type Culture Collection, Rockville, MD) was cultured in Roswell Park Memorial Institute medium 1640 (RPMI-1640), supplemented with 10% heat-inactivated FBS and 100 μg/ml of antibiotic (penicillin-streptomycin)**.**

Parasites. Pathogenic *Leishmania donovani* [MHOM/IN/1983/AG83] infection was maintained by the passage in BALB/c mice. *L. donovani* promastigotes, attained from infected BALB/c mice spleen were cultured in complete M199 media (10% FBS, pH 7.4, 100U/ml penicillin G sodium, 100 μg/ml streptomycin sulfate, 25 mM HEPES, sodium bicarbonate (2.2g/L), 10% FBS and 1% Pen Strep (pH - 7.2-7.4) at 22°C. All pathogen and animal-related works were performed according to prior approval from Institutional Biosafety Committee, CSIR-Indian Institute of Chemical Biology (CSIR IICB/IBSC/CERT-32/18-19) and CSIR-

IICB-Animal Ethics Committee (IICB/AEC/Meeting/Oct/ 2017), respectively. The care and maintenance of animals were done in agreement with the Committee for the Purpose of Control And Supervision of Experiments on Animals (CPCSEA), guidelines.

Parasite infection and treatment. A ratio of 1:10 (MΦs: parasite) was used to infect macrophages with *L. donovani* promastigotes. MΦs were incubated with parasites for 4 h, washed with PBS, and either fresh media was added or treated with inhibitors for the required time. To study the anti-leishmanial activity, normal and infected macrophages were treated with Spergulin-A at effective concentrations up to 72 h. Miltefosine used as a positive anti-leishmanial reference.

FACS and Confocal microscopy with CFSE tagged *L. donovani.* MΦs were parasitized with CFSE-tagged promastigotes (25 μM/1×10^6 promastigotes in 1 ml media for 30 min) and subjected to treatment with Spergulin-A (10, 20, 30 μg/ml)for 24 h.

For confocal microscopy, MΦs (1×10^5/glass coverslips) were washed twice with PBS after infection and treatment, then fixed in chilled 70% ethanol. The nuclei were stained with DAPI and observed under Olympus Fluoview FV10i confocal microscope with a 60X objective lens. For FACS, MΦs (1×10^5/well in a six-well plate) were rinsed twice with PBS after infection and treatment, harvested by scraping, resuspended in 400 μl PBS, and analyzed by BD FACS LSR Fortessa with excitation at 494 nm and emission at 518 nm.

Measurement of Phospho-P_{38}MAPK, Gp91-phox, Phospho-NF-κBp65. For phospho-P_{38}MAPK and Phospho-NF-κBp65 determination control, infected, and treated cells were washed with PBS, then fixed with 70% ethanol, after perforation with Triton-x 100 solution (0.5%) labeled with primary and respective fluorochrome conjugated antibodies. 20μM of SB203580 was used to inhibit p-P_{38}MAPK and 25 μM of curcumin for was used as A p-NF-κBp65 inhibitor with the necessary time of incubation periods. For the measurement of Gp91-phox, the above procedures were followed with specific primary and secondary antibodies.

Cells were then analyzed in BD FACS LSR Fortessa.

Measurement of P2x7 with BBG. To determine $P2X_7$ level control, infected, and treated cells were washed with PBS, then fixed with 70% ethanol, after perforation with Triton-x 100 solution (0.5%) labeled with primary and respective fluorochrome conjugated antibodies. Before treatment with Spergulin-A, cells were treated with 10µM of Brilliant Blue G (BBG) to inhibit $P2X_7$ in macrophage cells for 24 h of the incubation period.

Confocal Microscopy. After fixation with 70% ethanol and perforation, MΦs were stained with primary and fluorochrome conjugated secondary antibody. Then slides were mounted and nuclei were stained with DAPI in case of translocation of p-P_{38}MAPK, $P2X_7$, and Gp91-phox. To study the leishmanicidal activity, CFSE was used to stain *L. donovani* and Lysotracker was used to monitor acidic organelles in cells. Rab5 and CathepsinD were stained using primary and respective fluorochrome conjugated secondary antibodies. All specimens were observed under an Olympus Fluoview FV10i confocal microscope with a 60X objective lens.

Measurement of calcium release. Treated and untreated MΦs were collected, after washing twice with PBS, treated with FURA 2 AM (Molecular Probes) at 37ºC. After 45 min of incubation, the cells were washed with PBS, resuspended in fresh PBS, and examined by BD FACS LSR Fortessa with an excitation wavelength of 380 nm and an emission wavelength of 510 nm.

FACS analyses of intracellular ROS and NO. Intracellular ROS was monitored based on the transform in fluorescence of H2DCFDA. DAF-2 DA was used to perceive intracellular NO.[5] Briefly, after infection and treatment, MΦs were scrapped and incubated in PBS containing 7.0 µM DAF-2DA (at 37°C for 30 min) or 20 µM DCF-DA (at 37°C for 15 min) and evaluated by BD FACS LSR Fortessa with excitation at 480 nm and emission at 515 nm for both.

***In vivo* leishmanicidal activity.** To study leishmanicidal activity, parasite burdens in the spleen and bone marrow of control and Spergulin-A treated mice were determined. After

confirmation of the *L. donovani* infection in the BALB/c and given an adequate time of the infection propagation in vital organs like liver, spleen and bone marrow, infected mice were divided into two groups arbitrarily with one control group. For phospho-P38 MAPK, phospho-NF-κBp65 and $P2X_7$ protein determination, control and treated primary cells were stained using primary and fluorochrome conjugated secondary antibodies. Then Cells were then analyzed by BD FACS LSR Fortessa with respective excitation and emission wavelength.

In silico analysis. Molecular docking study[63,65] was employed to check the binding mode of the investigated compound toward its putative target $P2X_7R$. Chem 3D ultra 8.0.3 (Chem 3D Pro Version 8.0 And Chem Draw Ultra Version 8.0) software was used to construct the three-dimensional structure of the investigated compound.[66] The energy minimization of the compound was done by molecular orbital package (MOPAC) module with 100 iterations and a minimum RMS gradient of 0.10.[64] The preparation of the ligand structure prior to docking is performed by incorporating polar hydrogen atoms along with Gasteiger partial charges. The torsions are allowed to rotate during docking.[67]

The crystallographic structures of P2X7 (PDB: 5U1X) were used for this analysis.[68] The macromolecules were prepared by using Discovery Studio 3.0.[70] Polar hydrogen atoms were added to the protein by using the AutoDock Tools (ADT).[71] The grid box was selected 5U1X centered at the corresponding ligand crystal structure by maintaining a spacing of 1 Å.[64] Finally, the docking was performed by using the AutoDock Vina.[72] The docked poses were visualized in Discovery Studio 3.0.[70]

Statistical analysis. All experimental values were denoted as mean ± SEM acquired from at least three replicate experiments. Statistical significance and variations among groups were evaluated with One-Way analysis of variance (ANOVA) followed by Dunnett's test. P values ≤ 0.05 (*) or ≤ 0.01 (**) were considered as indicative of significance.

References

1. Tiuman, T.S., Santos, A.O., Ueda-Nakamura, T., Filho, B.P. & Nakamura, C.V. Recent advances in leishmaniasis treatment. *Int. J. Infect. Dis.* **15,** e525–e532 (2011).
2. Banerjee, S. et al. Attenuated Leishmania induce pro-inflammatory mediators and influence leishmanicidal activity by p38 MAPK dependent phagosome maturation in *Leishmania donovani* co-infected macrophages. *Sci. Rep*. **6,** 22335 (2016).
3. Alvar, J. et al. Leishmaniasis worldwide and global estimates of its incidence. *PLoS One* **7,** e35671 (2012).
4. Freitas, E.O., Leoratti, F.M.S., Freire-de-Lima, C.G., Morrot, A. & Feijó, D.F. The contribution of immune evasive mechanisms to parasite persistence in visceral leishmaniasis. *Front. Immunol.* **7,** 153 (2016).
5. Banerjee, S. et al. Intracellular anti-leishmanial effect of Spergulin-A, a triterpenoid saponin of *Glinus oppositifolius*. *Infect. Drug Resist.* **12**, 2933–2942 (2019).
6. Oryan, A. Plant-derived compounds in treatment of leishmaniasis. *Iran. J Vet. Res.* **16,** 1–19 (2015).
7. Kaur, H., Thakur, A. & Kaur, S. Immunoprophylactic potential of a cocktail of three low molecular weight antigens of *Leishmania donovani* along with various adjuvants against experimental visceral leishmaniasis. *Iran. J. Parasitol.* **13,** 11–23 (2018).
8. Mandal, N. et al. A triterpenoid saponin possessing antileishmanial activity from the leaves of *Careya arborea*. *Phytochemistry* **67,** 183–190 (2006).
9. Delmas, F. et al. Antileishmanial activity of three saponins isolated from ivy, a-hederin, b-hederin and hederacolchiside A1, as compared to their action on mammalian cells cultured in vitro. *Planta Med.* **66**, 343–347 (2000).

10. Maes, L. et al. In vitro and in vivo activities of a triterpenoid saponin extract (PX-6518) from the plant *Maesa balansae* against visceral leishmania species. *Antimicrob. Agents Chemother*. **48**, 130–136 (2004).

11. Miller, C.M. et al. The Role of the P2X7 Receptor in Infectious Diseases. *PLoS Pathog.* **7,** e1002212 (2011).

12. Aga, E. et al. Inhibition of the spontaneous apoptosis of neutrophil granulocytes by the intracellular parasite *Leishmania major*. *J. Immunol.* **169**, 898–905 (2002).

13. Lees, M.P. et al. P2X7 receptor-mediated killing of an intracellular parasite, *Toxoplasma gondii* by human and mouse macrophages. *J. Immunol.* **184**, 7040–7046 (2010).

14. Eskra, L., Mathison, A. & Splitter, G. Microarray analysis of mRNA levels from RAW 264.7 macrophages infected with *Brucella abortus*. *Infect. Immun.* **71**, 1125–1133 (2003).

15. Liu, J., Enomoto, S., Lancto, C.A., Abrahamsen, M.S. & Rutherford, M.S. Inhibition of apoptosis in *Cryptosporidium parvum*-infected intestinal epithelial cells is dependent on surviving. *Infect. Immun.* **76**, 3784–3792 (2008).

16. del Aguila, C. et al. *Encephalitozoon microsporidia* modulates p53-mediated apoptosis in infected cells. *Int. J. Parasitol.* **36**, 869–876 (2006).

17. Chen, S. et al. P2X7 receptor antagonism inhibits p38 MAPK activation and ameliorates neuronal apoptosis after subarachnoid hemorrhage in the rat. *Crit. Care Med.* **41**, e466-74. (2013).

18. Pfeiffer, Z.A. et al. Nucleotide receptor signalling in murine macrophages is linked to reactive oxygen species generation. *Free Radic. Biol. Med.* **42,** 1506–1516 (2007).

19. Gavala, M.L., Pfeiffer, Z.A. & Bertics, P.J. The nucleotide receptor P2RX7 mediates ATP-induced CREB activation in human and murine monocytic cells. *J. Leukoc. Biol.* **84,** 1159–1171 (2008).

20. Lee S.H. et al. Fucofuroeckol-A from *Eisenia bicyclis* inhibits inflammation in lipopolysaccharide-induced mouse macrophages via downregulation of the MAPK/NF-κB Signaling Pathway. *J. Chem.* **2016**, 6509212 (2016).

21. Cavalli, V. et al. The stress induced MAP kinase p38 regulates endocytic trafficking via GDI:Rab5 complex. *Mol. Cell.* **7**, 421–432 (2001).

22. Prive, C. & Descoteaux, A. *Leishmania donovani* promastigotes evade the activation of mitogen-activated protein kinases p38, c-Jun N-terminal kinase, and extracellular signal-regulated kinase-1/2 during infection of naive macrophages. *Eur. J. Immunol.* **30,** 2235–2244 (2000).

23. Jeong, H.J. et al. Inhibition of TNF-alpha and IL-6 production by Aucubin through blockade of NF-kappaB activation RBL-2H3 mast cells. Cytokine **18,** 252–259 (2002).

24. Junghae, M. & Raynes, J. G. Activation of p38 mitogen-activated protein kinase attenuates *Leishmania donovani* infection in macrophages. *Infect. Immun.* **70,** 5026–5035 (2002).

25. Gutierrez, M.G. Functional role(s) of phagosomal Rab GTPases. *Small GTPases* **4**, 148–158 (2013).

26. Fischer, W., Urban, N., Immig, K., Franke, H. & Schaefer, M. Natural compounds with P2X7 receptor-modulating properties. *Purinergic Signal.* **10,** 313–326 (2014).

27. Bartlett, R., Stokes, L. & Sluyter, R. The P2X7 receptor channel: recent developments and the use of P2X7 antagonists in models of disease. *Pharmacol. Rev.* **66**, 638–675 (2014).

28. Stokes, L., Layhadi, J.A., Bibic, L., Dhuna, K. & Fountain, S.J. P2X4 Receptor Function in the Nervous System and Current Breakthroughs in Pharmacology. *Front Pharmacol.* **8**, 291 (2017).

29. Helliwell, R.M. et al. Selected ginsenosides of the protopanaxdiol series are novel positive allosteric modulators of P2X7 receptors. *Br. J. Pharmacol.* **172**, 3326–3340 (2015).

30. Orioli, E., De Marchi, E., Giuliani, A.L. & Adinolfi, E. P2X7 Receptor Orchestrates Multiple Signalling Pathways Triggering Inflammation, Autophagy and Metabolic/Trophic Responses. *Curr Med Chem.* 24, 2261-2275 (2017).

31. Santos, J.A.A. et al. Effect of *Rheedia longifolia* Leaf Extract and Fractions on the $P2X_7$ Receptor *In Vitro*: Novel Antagonists? *J. Med. Food* **14**, 920-929 (2011).

32. Podolak, I., Galanty, A. & Sobolewska, D. Saponins as cytotoxic agents: a review. *Phytochem. Rev.* **9**, 425–474 (2010).

33. Peng, W. et al. Systemic administration of an antagonist of the ATP-sensitive receptor P2X7 improves recovery after spinal cord injury. *Proc. Natl. Acad. Sci. USA* **106**, 12489–12493 (2009).

34. Wang, X.H., Xie, X., Luo, X.G., Shang, H. & He, Z.Y. Inhibiting purinergic P2X7 receptors with the antagonist brilliant blue G is neuroprotective in an intranigral lipopolysaccharide animal model of Parkinson's disease. *Mol. Med. Rep.* **15**, 768–776 (2017).

35. Soares-Bezerra, R.J. et al. An Improved Method for P2X7R Antagonist Screening. *PLoS ONE* **10**, e0123089 (2015).

36. Namovic, M.T., Jarvis, M.F. & Donnelly-Roberts, D. High throughput functional assays for P2X receptors. *Curr. Protoc. Pharmacol.* Chapter 9:Unit 9 15 (2012).

37. Biswas, D. et al. ATP induced autophagy is associated with rapid killing of intracellular mycobacteria within human monocytes/macrophages. *BMC Immunol.* **9,** 35 (2008).

38. Freitas, E.O., Leoratti, F.M.S., Freire-de-Lima, C.G., Morrot, A. & Feijó, D.F. The contribution of immune evasive mechanisms to parasite persistence in visceral leishmaniasis. *Front. Immunol.* **7**, 153 (2016).

39. Olivier, M., Gregory, D.J. & Forget, G. Subversion mechanisms by which *Leishmania* parasites can escape the host immune response: a signaling point of view. *Clin. Microbiol. Rev.* **18,** 293–305 (2005).

40. Van Assche, T., Deschacht, M., da Luz, R.A., Maes. L. & Cos, P. Leishmania-macrophage interactions: insights into the redox biology. *Free Radic. Biol. Med.* **51**, 337–351(2011).

41. Soulat, D. & Bogdan, C. Function of macrophage and parasite phosphatases in Leishmaniasis, *Front Immunol.* **8**, 1838 (2017).

42. Fischer, W., Urban, N., Immig, K., Franke, H. & Schaefer, M. Natural compounds with P2X7 receptor-modulating properties. *Purinergic Signal.* **10,** 313–326 (2014).

43. Coutinho-Silva, R. et al. Inhibition of chlamydial infectious activity due to P2X7R-dependent phospholipase D activation. *Immunity* **19**, 403–412 (2003).

44. Coutinho-Silva, R. & Ojcius, D.M. Role of extracellular nucleotides in the immune response against intracellular bacteria and protozoan parasites. *Microbes Infect.* **14,** 1271–1277 (2012).

45. Amaral, E.P. et al. Pulmonary infection with hypervirulent Mycobacteria reveals a crucial role for the P2X7 receptor in aggressive forms of tuberculosis. *PLoS Pathog.* **10**, e1004188 (2014).

46. Chaves, S.P. et al. Modulation of P2X7 purinergic receptor in macrophages by *Leishmania amazonensis* and its role in parasite elimination. *Microbes Infect.* **11,** 842–849 (2009).

47. Figliuolo, V.R. et al. The role of the P2X7 receptor in murine cutaneous leishmaniasis: aspects of inflammation and parasite control. *Purinergic Signal.* **13,** 143–152 (2017).

48. Nunes, P. & Demaurex, N. The role of calcium signaling in phagocytosis. *J. Leukoc. Biol.* **88**, 57–68 (2010).

49. Pinton, P., Giorgi, C., Siviero, R., Zecchini, E. & Rizzuto, R. Calcium and apoptosis: ER-mitochondria Ca^{2+} transfer in the control of apoptosis. *Oncogene* **27,** 6407–6418 (2008).

50. Moradin, N. & Descoteaux, A. *Leishmania* promastigotes: building a safe niche within macrophages. *Front. Cell Infect. Microbiol.* **2**, 121 (2012).

51. Swulius, M.T. & Waxham M.N. Ca(2+)/calmodulin-dependent protein kinases. *Cell Mol. Life Sci.* **65**, 2637–2657 (2008).

52. Corre, I., Paris, F. & Huot, J. The p38 pathway, a major pleiotropic cascade that transduces stress and metastatic signals in endothelial cells. Oncotarget. **8**, 55684–55714 (2017).

53. Calegari-Silva, T.C. et al. NF-κB-mediated repression of iNOS expression in *Leishmania amazonensis* macrophage infection. *Immunol. Lett.* **127**, 19–26 (2009).

54. Tarafdar, A. & Pula G. The role of nadph oxidases and oxidative stress in neurodegenerative disorders. *Int. J. Mol. Sci.* **19**, 3824 (2018).

55. McAdam, E. et al. Inducible nitric oxide synthase (iNOS) and nitric oxide (NO) are important mediators of reflux-induced cell signalling in esophageal cells. **33**, 2035–43 (2012).

56. Yu, L., Quinn, M.T., Cross, A.R. & Dinauer, M.C. Gp91(phox) is the heme binding subunit of the superoxide-generating NADPH oxidase. *Proc. Natl. Acad. Sci. USA.* **95**, 7993–7998 (1998).

57. Lenertz, L.Y., Gavala, M.L., Hill, L.M. & Bertics, P.J. Cell signaling via the P2X(7) nucleotide receptor: linkage to ROS production, gene transcription, and receptor trafficking. *Purinergic Signal.* **5**, 175–187 (2009).

58. Nakahira, K. et al. Autophagy proteins regulate innate immune responses by inhibiting the release of mitochondrial DNA mediated by the NALP3 inflammasome. *Nat. Immunol.* **12**, 222–230 (2011).

59. Carneiro, P.P. et al. The role of nitric oxide and reactive oxygen species in the killing of *Leishmania braziliensis* by monocytes from patients with cutaneous leishmaniasis. *PLoS ONE* **11**, e0148084 (2016).

60. Almeida, T.F., Palma, L.C., Mendez, L.C., Noronha-Dutra, A.A. & Veras, P.S. *Leishmania amazonensis* fails to induce the release of reactive oxygen intermediates by CBA macrophages. *Parasite Immunol.* **34**, 492–498 (2012).

61. Gantt, K.R. et al. Oxidative responses of human and murine macrophages during phagocytosis of *Leishmania chagasi*. *J. Immunol.* **167,** 893–901 (2001).

62. Bogdan, C., Rollinghoff, M. & Diefenbach A. The role of nitric oxide in innate immunity. *Immunol. Rev.* **173**, 17–26 (2000).

63. Amin, S.A. et al. Pharmacoinformatics study of piperolactam a from Piper beetle root as new lead for nonsteroidal anti fertility drug development. *Comput. Biol. Chem.* **67,** 213–224 (2017a).

64. Amin, S.A., Adhikari, N., Agrawal, R.K., Jha, T. & Gayen, S. Possible Binding Mode Analysis of Pyrazolo-triazole Hybrids as Potential Anticancer Agents through Validated Molecular Docking and 3D-QSAR Modeling Approaches. *Lett. Drug Des. Discov.* **14,** 515–527 (2017b).

65. Bhardwaj, B. et al. Insight into structural features of phenyltetrazole derivatives as ABCG2 inhibitors for the treatment of multidrug resistance in cancer. *SAR QSAR Environ. Res.* **30,** 457–475 (2019).

66. Chem 3D Pro Version 8.0 And Chem Draw Ultra Version 8.0 Are Software Programs Developed by Cambridge Soft Corporation. USA.

67. Lv, P.C. Li, H.Q., Sun, J., Zhou, Y. & Zhu, H.L. Synthesis and biological evaluation of pyrazole derivatives containing thiourea skeleton as anticancer agents. *Bioorg. Med. Chem.* **18,** 4606–4614 (2010).

68. https://www.rcsb.org/structure/5U1X: https://www.rcsb.org/structure/5U1X (as accessed on 14th August 2019)

69. Karasawa, A. & Kawate, T. Structural basis for subtype-specific inhibition of the P2X7 receptor. *Elife*. **5,** e22153 (2016).

70. Discovery Studio 3.0 (DS 3.0), Accelrys Inc., CA, USA, 2015.

71. Autodock Tools 1.5.6 (ADT)/MGL Tools 1.5.6, The Scripps Research Institute, CA, USA, 2012. Available at http://mgltools.scripps.edu

72. Trott, O. & Olson, A.J. AutoDock Vina: Improving the speed and accuracy of docking with a new scoring function, efficient optimization, and multithreading. *J. Comput. Chem.* 31, 455–461 (2010).

Acknowledgments

Sincere thanks are given to the Science and Engineering Research Board (SERB), Govt. of India (Grant No. PDF/2016/001437 and EMR/2015/001674) for financial support. The manuscript has been critically checked by the full version of the Grammarly software and Urkund for language corrections and plagiarism.

Author contributions

N.M., K.D.S., and S.B. conceptualize the work, N.M., and S.B. acquired, analyzed and written the biological data. S.A.A. and T.J. acquired and analyzed the in silico binding assay data. N.M., S.B. and SAA wrote the manuscript. N.M., T.J, S.D., and K.D.S. supervised the work.

Figure Captions

Fig. 1 Evaluation of $P2X_7$ receptor involvement in the intracellular anti-leishmanial activity of Spergulin-A. **a** Spergulin-A reduces intracellular *L. donovani* expressed as the number of parasites/20 MΦs dose-dependently after 24 h of treatment with miltefosine as positive control expressing its LC_{50} and LC_{90} values. **b** RAW 264.7 MΦ survivability in accordance with the $P2X_7$ receptor antagonist BB-G application after 24 h. **c** FACS monitored co-expression

analyses of CFSE-tagged *L. donovani* and subsequent $P2X_7R$ expression during infection and Spergulin-A (30µg/mL) treatment. **d** Bar diagram of Spergulin-A mediated intracellular leishmanial parasite removal and subsequent aversion by BB-G (10µM) application expressed as the number of parasites/20 MΦs. **e** Confocal micrographs of consequent expression of CFSE-tagged intracellular *L. donovani* with $P2X_7R$ expression during Spergulin-A (30µg/mL) and BB-G (10µM) application. Spergulin-A enhanced $P2X_7R$ expression and intracellular *L. Donovani* removal, whereas, BB-G caused reversal of the Spergulin-A mediated intracellular parasite removal and $P2X_7R$ over-expression. Scale bars, 10 µm. Images are representative of three separate experiments. All values are expressed as mean ± SEM from triplicate assays from three independent experiments (*P*-values ≤0.05 (*) or ≤0.01 (**) vs infected panel except for **b**, where the reference is the RAW 264.7 MΦs; ns denotes not significant).

Fig. 2 FACS monitored Ca^{++} influx evaluation with $P2X_7R$ expression analyses of *L. donovani* parasitized, Spergulin-A and BB-G exposed MΦs by Fura2M. **a** FACS analyses with $P2X_7R$ expression and Ca^{++} corresponding to Fura2M. The four quadrants represent different stages of $P2X_7R$ and Ca^{++} expressing populations, i.e. Q1 (only $P2X_7R$ expressing), Q2 (both $P2X_7R$ and Ca^{++} expressing), Q3 (double negative) and Q4 (only Ca^{++} expressing). **b** Mean fluorescence index values equivalent of the expressions of both $P2X_7R$ and Ca^{++} during *L. donovani* infection, Spergulin-A treatment, and BB-G application. **c** Percentage of $P2X_7R$ and Ca^{++} expressing RAW 264.7 MΦ cells against the parent population during *L. donovani* infection, Spergulin-A treatment and BB-G application. Images are representative of three separate experiments. All values are expressed as mean ± SEM from triplicate assays from three independent experiments (*P*-values ≤0.05 (*) or ≤0.01 (**) vs infected panel).

Fig. 3 P_{38}MAPK expression alteration with $P2X_7$ receptor involvement during Spergulin-A treatment. **a** Flow cytometric analyses of p-P_{38}MAPK expression alteration towards *L. donovani* infection, Spergulin-A treatment and P_{38}MAPK-inhibitor (SB203580) application

and their co-dependence in Spergulin-A mediated anti-leishmanial effect with the histogram of mean fluorescence values of p-P_{38}MAPK and CFSE-tagged intracellular *L. donovani* in respective populations. **b** Confocal micrographs of co-expression analyses of $P2X_7R$ and P_{38}MAPK in *L. donovani* parasitized, Spergulin-A and BB-G exposed MΦs. Scale bars, 10 μm. **c** NF-κBp65 expression alteration with $P2X_7$ receptor involvement during Spergulin-A treatment. Flow cytometric analyses of NF-κBp65 expression alteration towards *L. donovani* infection, Spergulin-A treatment and NF-κB-inhibitor (Curcumin) application and their co-dependence in Spergulin-A mediated anti-leishmanial effect with the histogram of mean fluorescence values of NF-κBp65 and CFSE-tagged intracellular *L. donovani* in respective populations. Images are representative of three separate experiments. All values are expressed as mean ± SEM from triplicate assays from three independent experiments (*P*-values ≤0.05 (*) or ≤0.01 (**) vs infected panel).

Fig. 4 a Evaluation of changes in ROS production in control, infected, and Spergulin-A (30 μg/mL) treated MΦs with H2DCFDA by FACS with or without NAC. **b** Intracellular NO production alterations were also examined with fluorescent probe DAF-2 DA in control, infected, and Spergulin-A (30 μg/mL) treated MΦs by FACS with or without NMMA. **c** Changes in CFSE-tagged intracellular *L. donovani* parasites were micrographed with respect to Spergulin-A treatment and co-application of NAC and NMMA for evaluation of ROS and NO involvement in Spergulin-A mediated anti-leishmanial effect by confocal microscopy, scale bars, 10 μm. Images are representative of three separate experiments. All values are expressed as mean ± SEM from triplicate assays from three independent experiments (*P*-values ≤0.05 (*) or ≤0.01 (**) vs infected panel).

Fig. 5 Co-expression alteration of p-P_{38}MAPK and Gp91-phox, p-NF-κBp65 and Gp91-phox in Spergulin-A mediated anti-leishmanial effect. **a** Spergulin-A at different doses (10, 20 and 30μg/mL) applied in the infected MΦs found to elevate levels of Gp91-phox for p-P_{38}MAPK

positive MΦs as evaluated by FACS. Histograms of percent parent populations for p-P_{38}MAPK positive MΦs and both Gp91-phox and p-P_{38}MAPK for different infected and Spergulin-A treated populations denoted their inter-connections. Spergulin-A at different doses (10, 20 and 30μg/mL) applied in the infected MΦs found to elevate levels of Gp91-phox for NF-κBp65 (Rel A) positive MΦs as evaluated by FACS. Histograms of percent parent populations for NF-κBp65 positive MΦs and both Gp91-phox and NF-κBp65 for different infected and Spergulin-A treated populations denoted their inter-connections. **b** Confocal microscopy elaborated that Gp91-phox expression was simultaneously up-regulated with increasing doses of Spergulin-A along with the increment of p-P_{38}MAPK expression. Images are representative of three separate experiments, scale bars, 10 μm. All values are expressed as mean ± SEM from triplicate assays from three independent experiments (*P*-values ≤0.05 (*) or ≤0.01 (**) vs infected panel).

Fig. 6 a Dynamics of phagolysosomal maturation in demonstrating the dose-dependent anti-leishmanial effect of Spergulin-A. Early phagosome marker Rab-5 expression got upregulated in the treated panel with respect to the control and infected panels. Cathepsin-D (Late phagolysosomal marker) expression also got upregulated with the exposure of Spergulin-A and signifies the phagolysosomal maturation process. Images are representative of three separate experiments, scale bars, 10 μm. **b** In vivo evaluation of the anti-leishmanial effect of Spergulin-A with P_{38}-MAPK and $P2X_7$ receptor involvement. Graphical presentation of the in-vivo treatment schedule and observation parameters. After confirmation of the *L. donovani* infection in the BALB/C mice, infected mice were divided into two groups arbitrarily with one control group. Control and treated groups received 30mg/kg b.wt. of Spergulin-A for every alternate day for 10 doses then sacrificed and spleen and bone marrow MΦs were harvested after treatment schedule and examined for $P2X_7R$, p-P_{38}MAPK and NF-κBp65 expression. Mice from each group were sacrificed and spleen MΦs were harvested for each group and evaluated

by flow cytometry for the linked expressions of $P2X_7R$-p-P_{38}MAPK and $P2X_7R$-NFκBp65. Mean fluorescence index values equivalent of the expressions of both $P2X_7R$- p-P_{38}MAPK and $P2X_7R$-NFκBp65 from spleen MΦs of different experimental mice groups. **c** Mice from each group were sacrificed and bone marrow MΦs were harvested from each group and evaluated by flow cytometry for the linked expressions of $P2X_7R$-p-P_{38}MAPK. Mean fluorescence index values equivalent of the expressions of both $P2X_7R$- p-P_{38}MAPK from bone marrow MΦs of different experimental mice groups. Images are representative of three separate experiments. All values are expressed as mean ± SEM from triplicate assays from three independent experiments (*P*-values ≤0.05 (*) or ≤0.01 (**) vs infected panel).

Fig. 7 In-silico docking study of the interdependence of Spergulin-A with P2X7 receptor. **a** The proposed interaction investigated compound Spergulin-A with the P2X7 receptor. The green-colored stick is the inbound crystal compound. **b** The proposed 3D interaction investigated compound Spergulin-A with the amino acid residues of the $P2X_7$ receptor. **c** The proposed 2D interaction investigated compound Spergulin-A with the amino acid residues of the $P2X_7$ receptor. **d** A graphical presentation of the step-wise anti-leishmanial activity propagation by Spergulin-A.

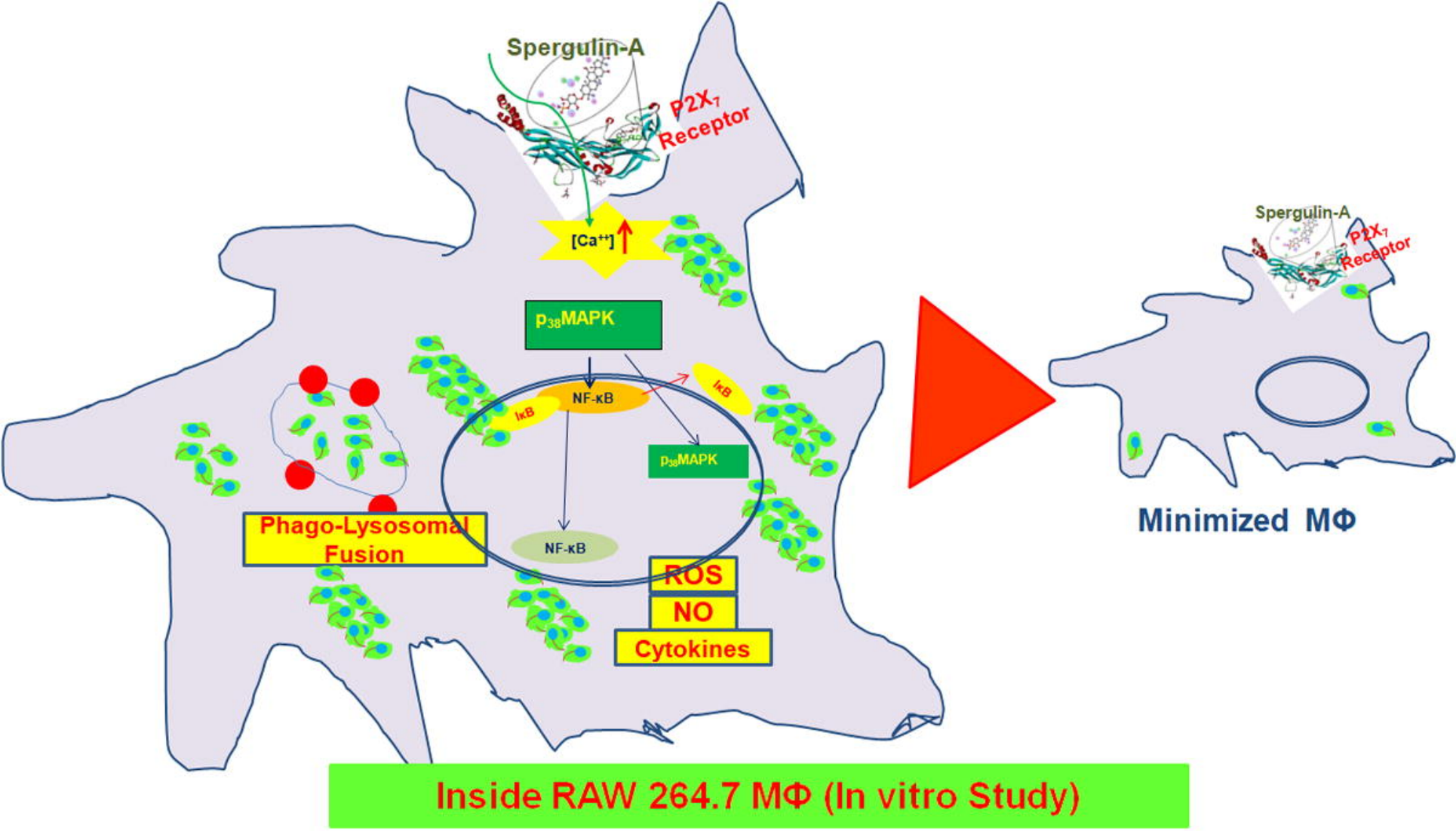
Spergulin-A
P2X7 Receptor
[Ca++]
p38MAPK
NF-κB
IκB
IκB
p38MAPK
NF-κB
Phago-Lysosomal Fusion
ROS
NO
Cytokines
Spergulin-A
P2X7 Receptor
Minimized MΦ
Inside RAW 264.7 MΦ (In vitro Study)

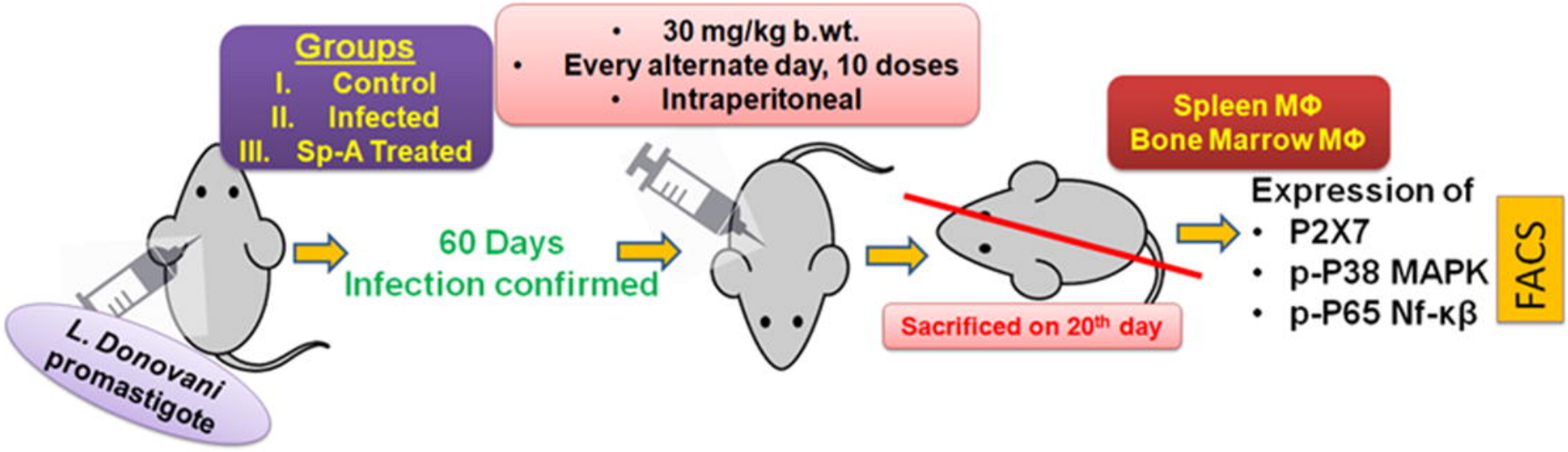
Groups
I. Control
II. Infected
III. Sp-A Treated
• 30 mg/kg b.wt.
• Every alternate day, 10 doses
• Intraperitoneal
L. Donovani promastigote
60 Days
Infection confirmed
Sacrificed on 20th day
Spleen MΦ
Bone Marrow MΦ
Expression of
• P2X7
• p-P38 MAPK
• p-P65 Nf-κβ
FACS
Inside Mice Spleen and Bone Marroe MΦ (In vivo confirmation)

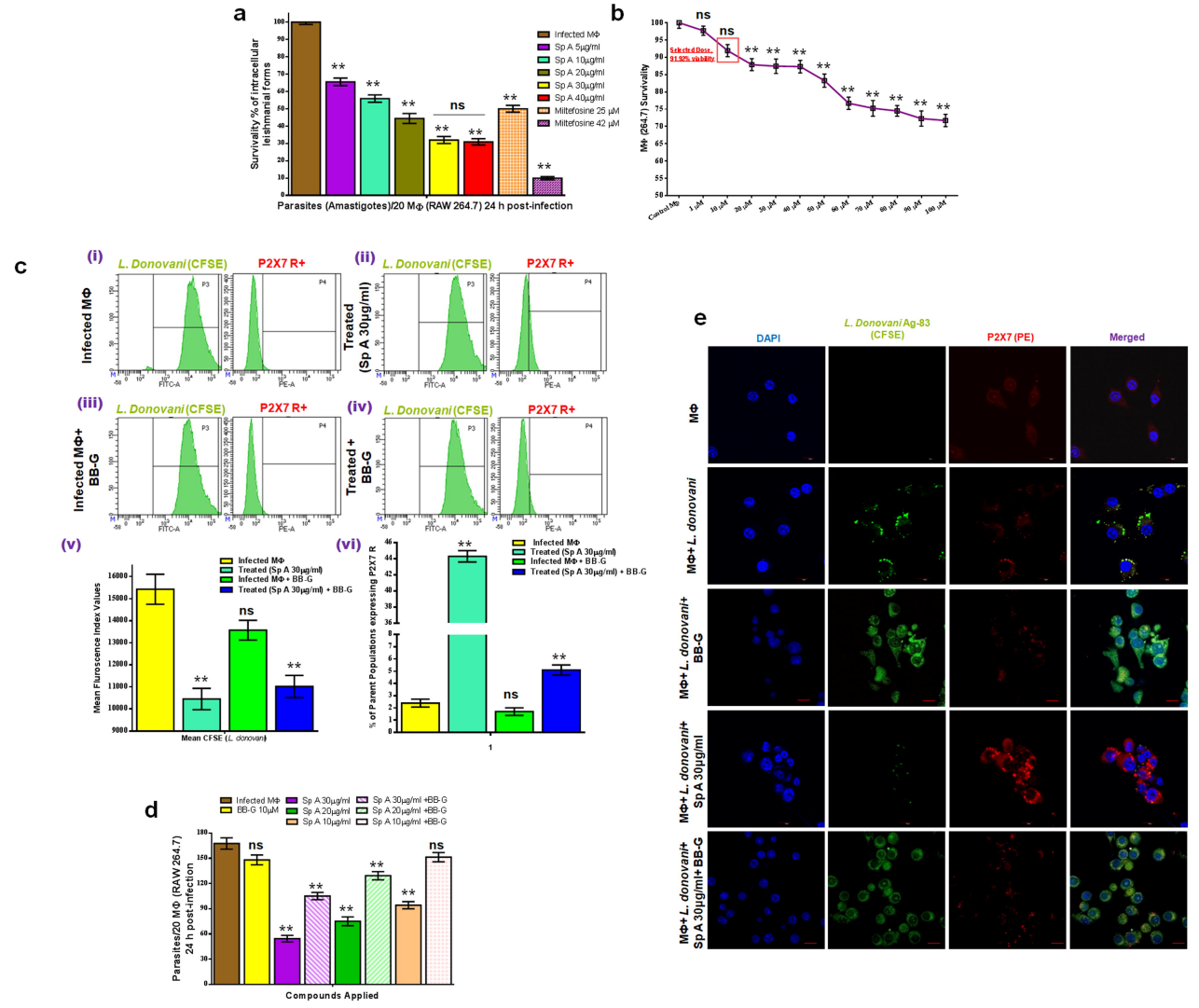
a
Survivality % of intracellular leishmanial forms
Parasites (Amastigotes)/20 MΦ (RAW 264.7) 24 h post-infection
Infected MΦ
Sp A 5μg/ml
Sp A 10μg/ml
Sp A 20μg/ml
Sp A 30μg/ml
Sp A 40μg/ml
Miltefosine 25 μM
Miltefosine 42 μM
ns
b
MΦ (264.7) Survivality
Selected Dose, 91.92% viability
Control MΦ
1 μM
10 μM
20 μM
30 μM
40 μM
50 μM
60 μM
70 μM
80 μM
90 μM
100 μM
c
(i)
L. Donovani (CFSE)
P2X7 R+
Infected MΦ
(ii)
Treated (Sp A 30μg/ml)
(iii)
Infected MΦ+ BB-G
(iv)
Treated + BB-G
FITC-A
PE-A
(v)
Mean Fluroscence Index Values
Mean CFSE (L. donovani)
Infected MΦ
Treated (Sp A 30μg/ml)
Infected MΦ+ BB-G
Treated (Sp A 30μg/ml) + BB-G
(vi)
% of Parent Populations expressing P2X7 R
d
Parasites/20 MΦ (RAW 264.7) 24 h post-infection
Compounds Applied
Infected MΦ
BB-G 10μM
Sp A 30μg/ml
Sp A 20μg/ml
Sp A 10μg/ml
Sp A 30μg/ml +BB-G
Sp A 20μg/ml +BB-G
Sp A 10μg/ml +BB-G
e
DAPI
L. Donovani Ag-83 (CFSE)
P2X7 (PE)
Merged
MΦ
MΦ+ L. donovani
MΦ+ L. donovani+ BB-G
MΦ+ L. donovani+ Sp A 30μg/ml
MΦ+ L. donovani+ Sp A 30μg/ml+ BB-G

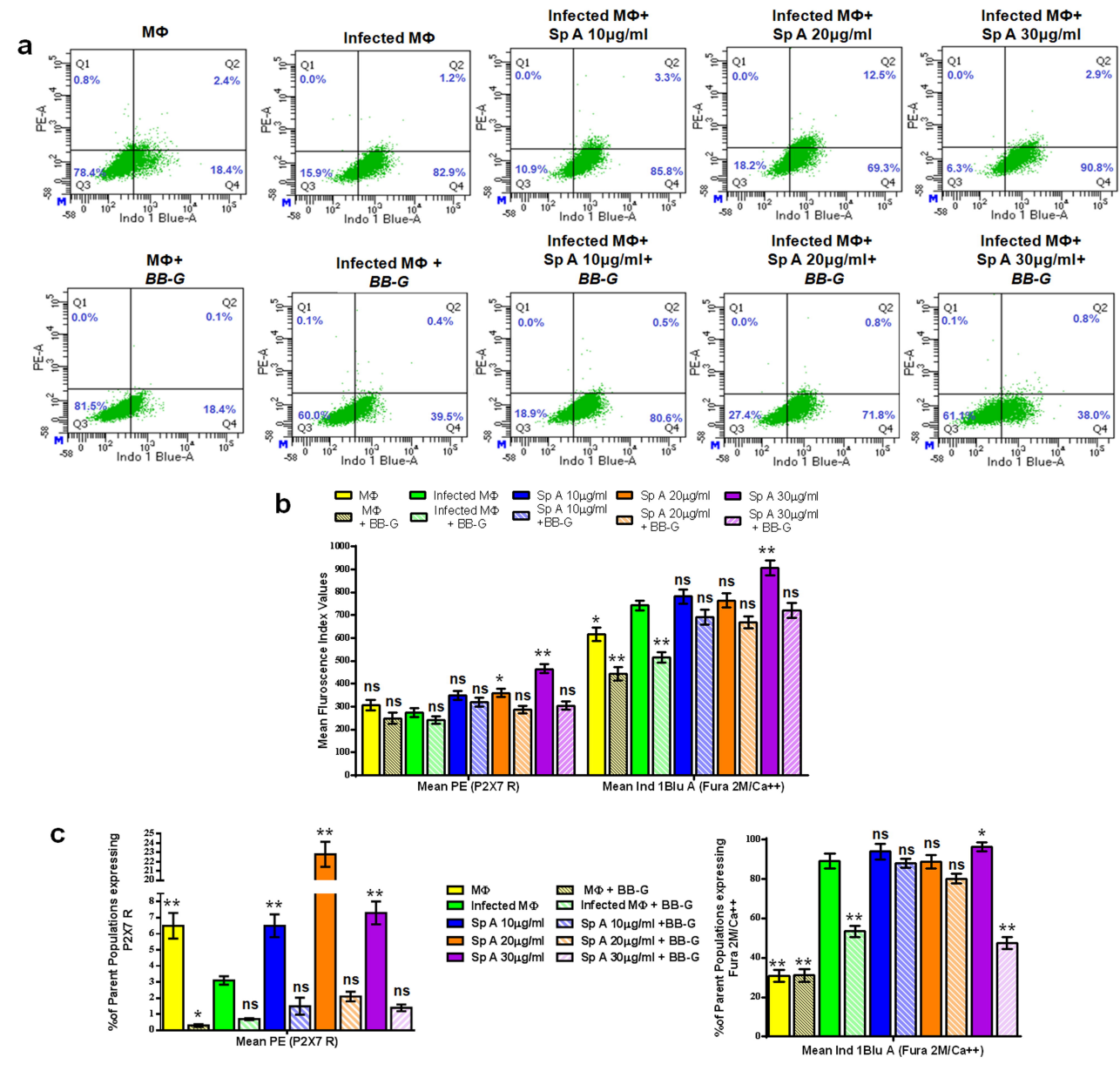
a
MΦ
Q1 0.8%
Q2 2.4%
Q3 78.4%
Q4 18.4%
Infected MΦ
Q1 0.0%
Q2 1.2%
Q3 15.9%
Q4 82.9%
Infected MΦ+ Sp A 10µg/ml
Q1 0.0%
Q2 3.3%
Q3 10.9%
Q4 85.8%
Infected MΦ+ Sp A 20µg/ml
Q1 0.0%
Q2 12.5%
Q3 18.2%
Q4 69.3%
Infected MΦ+ Sp A 30µg/ml
Q1 0.0%
Q2 2.9%
Q3 6.3%
Q4 90.8%
MΦ+ BB-G
Q1 0.0%
Q2 0.1%
Q3 81.5%
Q4 18.4%
Infected MΦ + BB-G
Q1 0.1%
Q2 0.4%
Q3 60.0%
Q4 39.5%
Infected MΦ+ Sp A 10µg/ml+ BB-G
Q1 0.0%
Q2 0.5%
Q3 18.9%
Q4 80.6%
Infected MΦ+ Sp A 20µg/ml+ BB-G
Q1 0.0%
Q2 0.8%
Q3 27.4%
Q4 71.8%
Infected MΦ+ Sp A 30µg/ml+ BB-G
Q1 0.1%
Q2 0.8%
Q3 61.1%
Q4 38.0%
PE-A
Indo 1 Blue-A
b
MΦ
MΦ + BB-G
Infected MΦ
Infected MΦ + BB-G
Sp A 10µg/ml
Sp A 10µg/ml +BB-G
Sp A 20µg/ml
Sp A 20µg/ml + BB-G
Sp A 30µg/ml
Sp A 30µg/ml + BB-G
Mean Fluroscence Index Values
Mean PE (P2X7 R)
Mean Ind 1Blu A (Fura 2M/Ca++)
c
%of Parent Populations expressing P2X7 R
Mean PE (P2X7 R)
%of Parent Populations expressing Fura 2M/Ca++
Mean Ind 1Blu A (Fura 2M/Ca++)

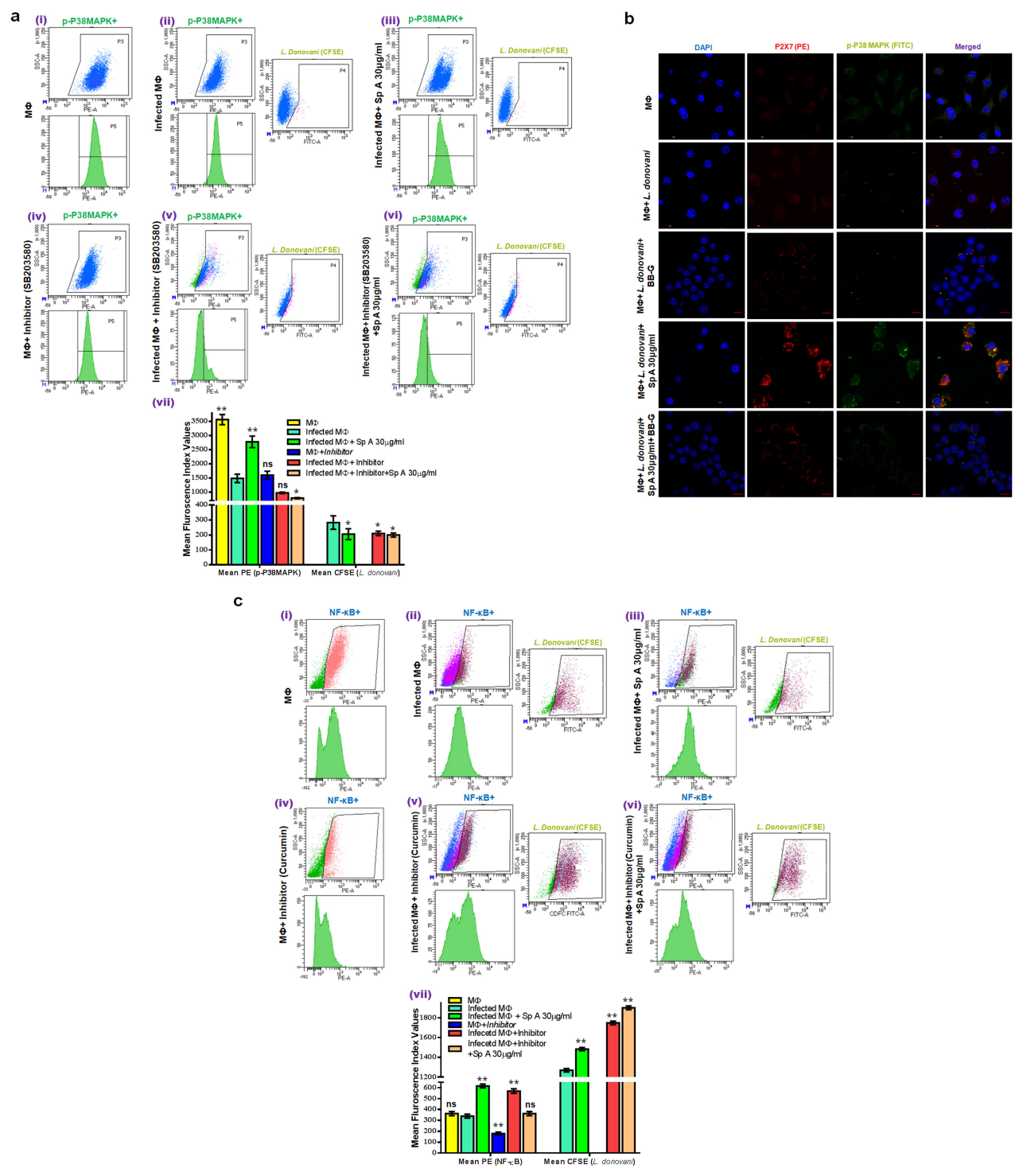
a
(i) p-P38MAPK+
(ii) p-P38MAPK+
(iii) p-P38MAPK+
(iv) p-P38MAPK+
(v) p-P38MAPK+
(vi) p-P38MAPK+
MΦ
Infected MΦ
Infected MΦ+ Sp A 30µg/ml
MΦ+ Inhibitor (SB203580)
Infected MΦ + Inhibitor (SB203580)
Infected MΦ+Inhibitor(SB203580) +Sp A 30µg/ml
L. Donovani (CFSE)
P3
P4
P5
SSC-A
PE-A
FITC-A
(vii)
Mean Fluroscence Index Values
MΦ
Infected MΦ
Infected MΦ + Sp A 30µg/ml
MΦ+Inhibitor
Infected MΦ+Inhibitor
Infected MΦ+Inhibitor+Sp A 30µg/ml
ns
Mean PE (p-P38MAPK)
Mean CFSE (L. donovani)
b
DAPI
P2X7 (PE)
p-P38 MAPK (FITC)
Merged
MΦ
MΦ+ L. donovani
MΦ+ L. donovani+ BB-G
MΦ+ L. donovani+ Sp A 30µg/ml
MΦ+ L. donovani+ Sp A 30µg/ml+ BB-G
c
(i) NF-κB+
(ii) NF-κB+
(iii) NF-κB+
(iv) NF-κB+
(v) NF-κB+
(vi) NF-κB+
MΦ
Infected MΦ
Infected MΦ+ Sp A 30µg/ml
MΦ+ Inhibitor (Curcumin)
Infected MΦ+ Inhibitor (Curcumin)
Infected MΦ+ Inhibitor (Curcumin) +Sp A 30µg/ml
L. Donovani (CFSE)
CDFC FITC-A
(vii)
Mean Fluroscence Index Values
MΦ
Infected MΦ
Infected MΦ + Sp A 30µg/ml
MΦ+Inhibitor
Infected MΦ+Inhibitor
Infecetd MΦ+Inhibitor +Sp A 30µg/ml
ns
Mean PE (NF-κB)
Mean CFSE (L. donovani)

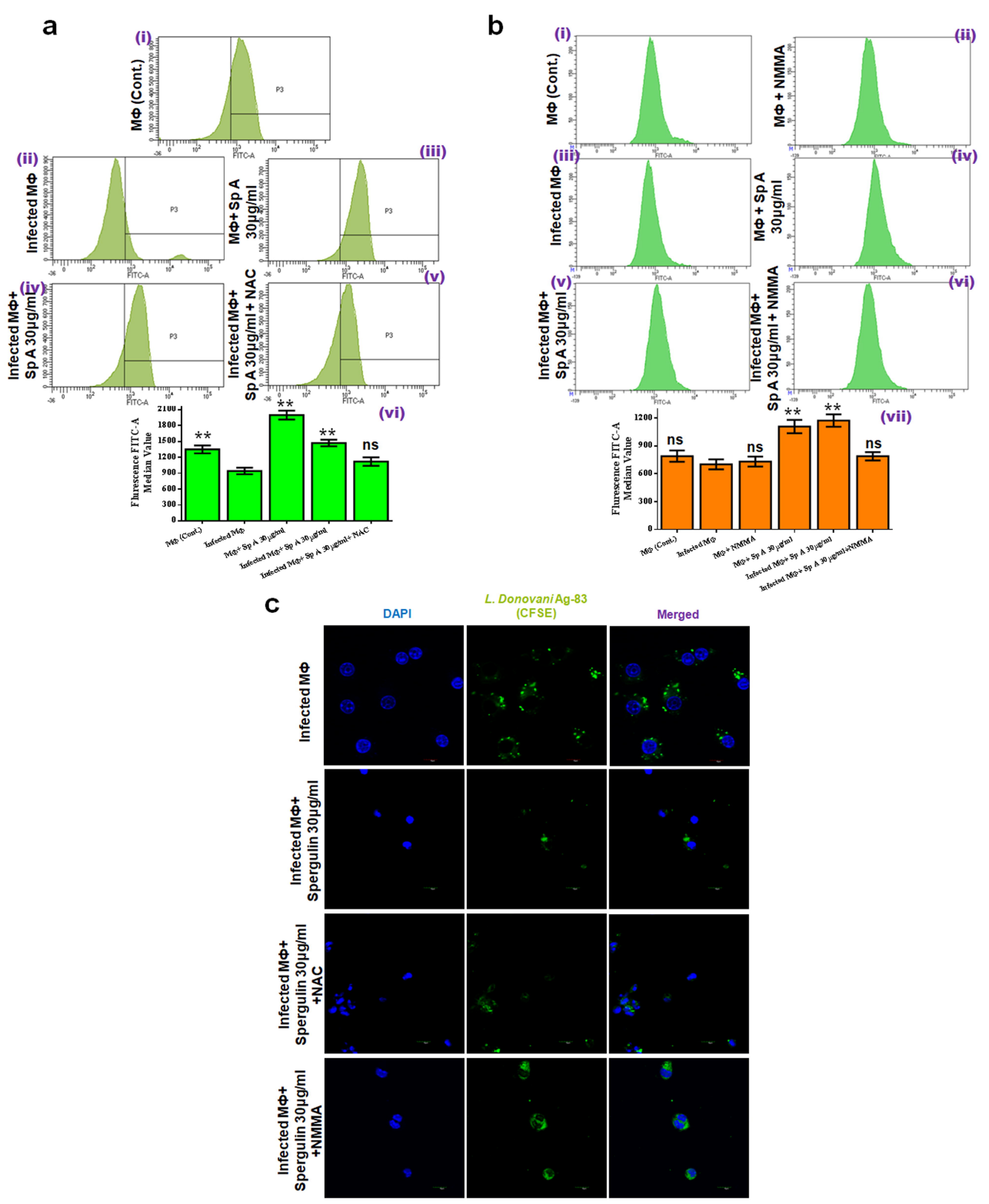
a
(i)
MΦ (Cont.)
(ii)
Infected MΦ
(iii)
MΦ+ Sp A 30µg/ml
(iv)
Infected MΦ+ Sp A 30µg/ml
(v)
Infected MΦ+ Sp A 30µg/ml + NAC
P3
FITC-A
(vi)
Flurescence FITC-A Median Value
**
**
**
ns
MΦ (Cont.)
Infected MΦ
MΦ+ Sp A 30 µg/ml
Infected MΦ+ Sp A 30 µg/ml
Infected MΦ+ Sp A 30 µg/ml + NAC
b
(i)
MΦ (Cont.)
(ii)
MΦ + NMMA
(iii)
Infected MΦ
(iv)
MΦ + Sp A 30µg/ml
(v)
Infected MΦ+ Sp A 30µg/ml
(vi)
Infected MΦ+ Sp A 30µg/ml + NMMA
(vii)
Flurescence FITC-A Median Value
ns
ns
**
**
ns
MΦ (Cont.)
Infected MΦ
MΦ + NMMA
MΦ+ Sp A 30 µg/ml
Infected MΦ+ Sp A 30 µg/ml
Infected MΦ+ Sp A 30 µg/ml+NMMA
c
DAPI
L. Donovani Ag-83 (CFSE)
Merged
Infected MΦ
Infected MΦ+ Spergulin 30µg/ml
Infected MΦ+ Spergulin 30µg/ml +NAC
Infected MΦ+ Spergulin 30µg/ml +NMMA

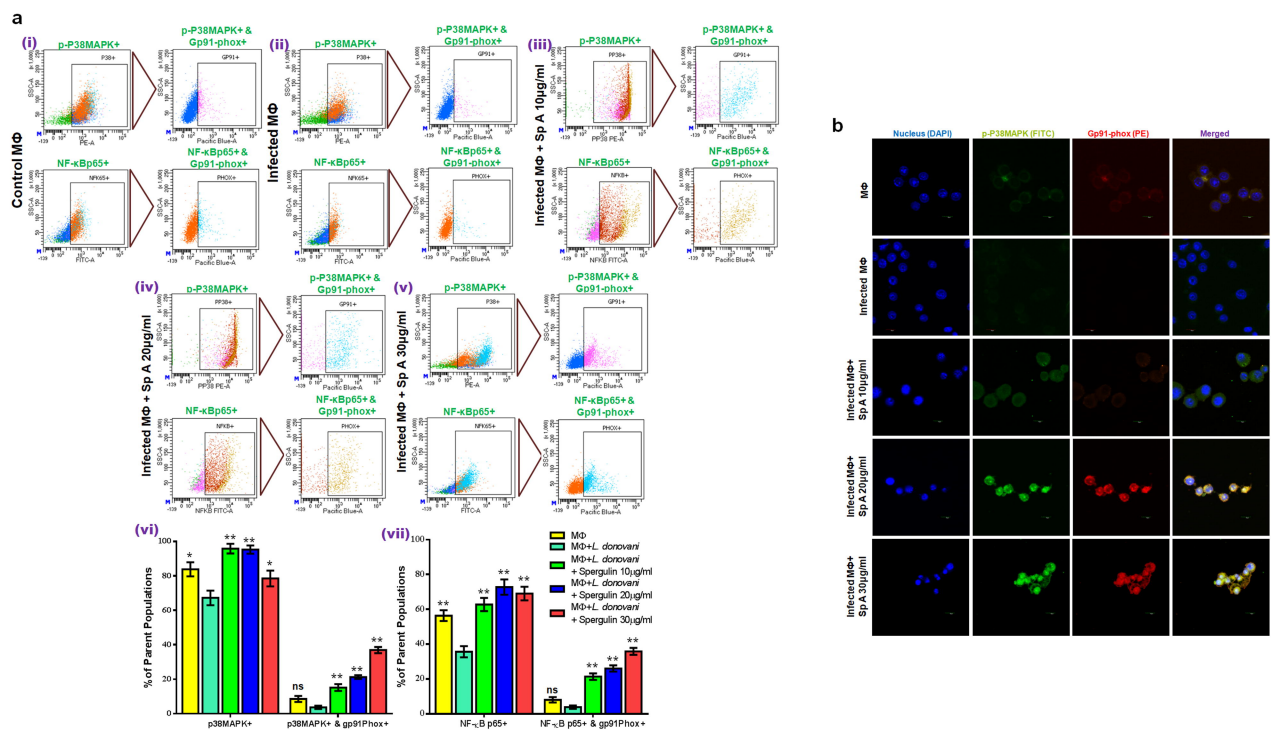
a
(i)
Control MΦ
p-P38MAPK+
p-P38MAPK+ & Gp91-phox+
NF-κBp65+
NF-κBp65+ & Gp91-phox+
(ii)
Infected MΦ
(iii)
Infected MΦ + Sp A 10μg/ml
(iv)
Infected MΦ + Sp A 20μg/ml
(v)
Infected MΦ + Sp A 30μg/ml
(vi)
% of Parent Populations
p38MAPK+
p38MAPK+ & gp91Phox+
ns
(vii)
NF-κB p65+
NF-κB p65+ & gp91Phox+
MΦ
MΦ+L. donovani
MΦ+L. donovani + Spergulin 10μg/ml
MΦ+L. donovani + Spergulin 20μg/ml
MΦ+L. donovani + Spergulin 30μg/ml
b
Nucleus (DAPI)
p-P38MAPK (FITC)
Gp91-phox (PE)
Merged
MΦ
Infected MΦ
Infected MΦ+ Sp A 10μg/ml
Infected MΦ+ Sp A 20μg/ml
Infected MΦ+ Sp A 30μg/ml

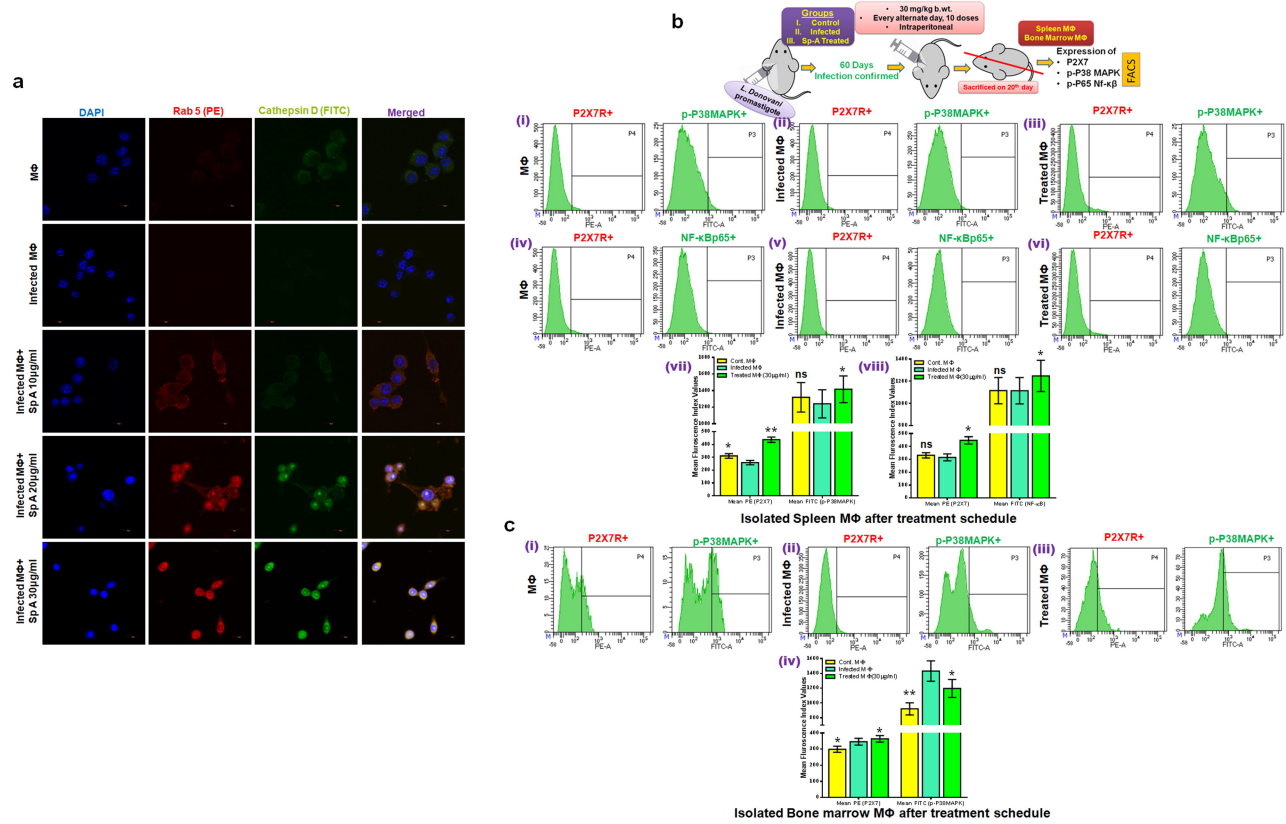
a
DAPI
Rab 5 (PE)
Cathepsin D (FITC)
Merged
MΦ
Infected MΦ
Infected MΦ+ SpA 10µg/ml
Infected MΦ+ SpA 20µg/ml
Infected MΦ+ SpA 30µg/ml
b
Groups
I. Control
II. Infected
III. Sp-A Treated
L. Donovani promastigote
60 Days Infection confirmed
30 mg/kg b.wt.
Every alternate day, 10 doses
Intraperitoneal
Sacrificed on 20th day
Spleen MΦ
Bone Marrow MΦ
Expression of
P2X7
p-P38 MAPK
p-P65 Nf-κβ
FACS
P2X7R+
p-P38MAPK+
NF-κBp65+
Isolated Spleen MΦ after treatment schedule
Cont. MΦ
Infected MΦ
Treated MΦ (30µg/ml)
Mean Fluorescence Index Values
Mean PE (P2X7)
Mean FITC (p-P38MAPK)
Mean FITC (NF-κB)
c
Isolated Bone marrow MΦ after treatment schedule

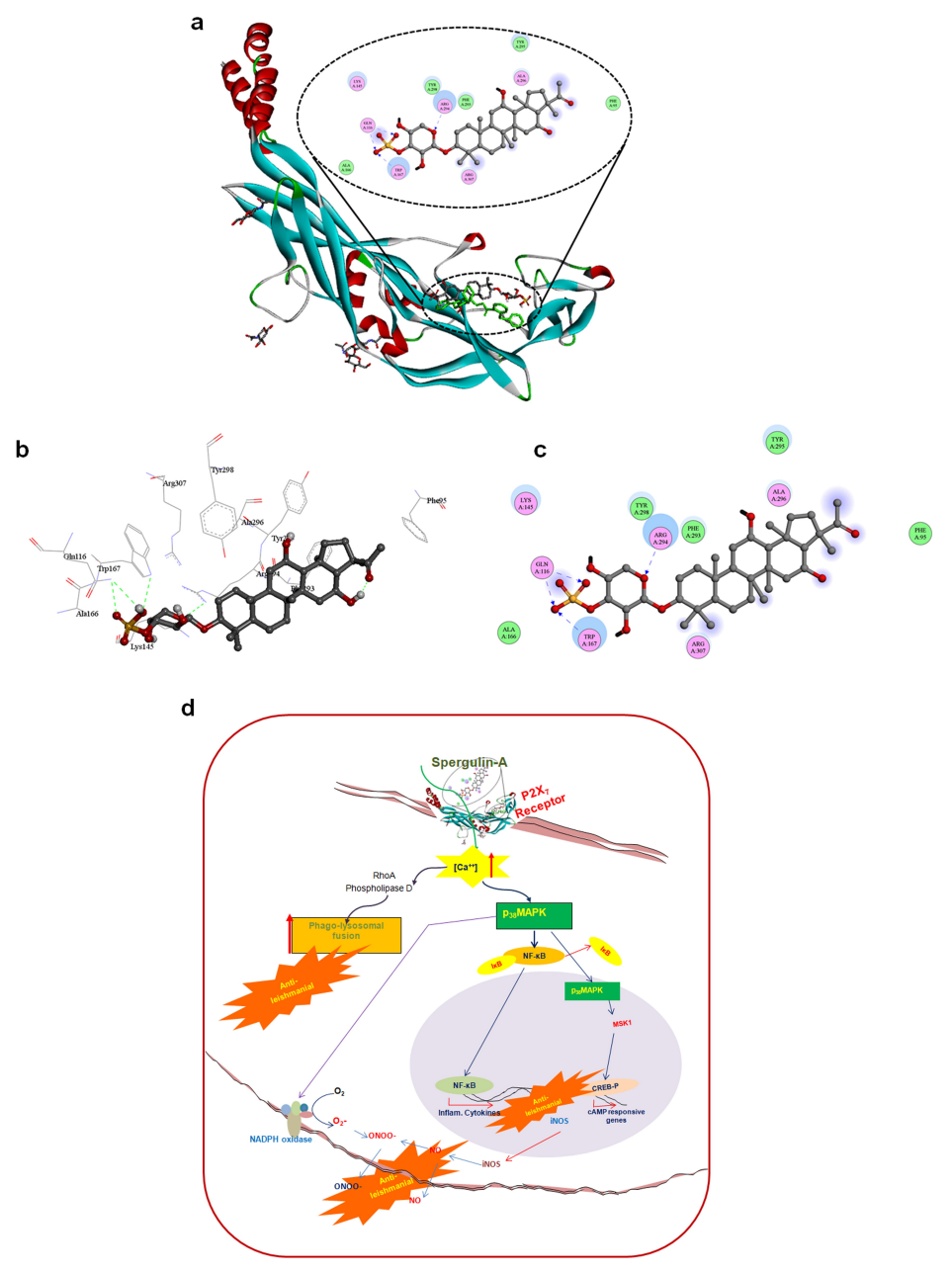
a
b
Tyr298
Arg307
Phe95
Ala296
Tyr295
Gln116
Trp167
Ala166
Lys145
Arg294
Phe293
c
TYR A:295
LYS A:145
TYR A:298
ALA A:296
ARG A:294
PHE A:293
PHE A:95
GLN A:116
ALA A:166
TRP A:167
ARG A:307
d
Spergulin-A
P2X7 Receptor
[Ca++]
RhoA
Phospholipase D
p38MAPK
Phago-lysosomal fusion
Anti-leishmanial
NF-κB
IκB
IκB
p38MAPK
MSK1
NF-κB
Inflam. Cytokines
Anti-leishmanial
CREB-P
cAMP responsive genes
iNOS
O2
O2-
NADPH oxidase
ONOO-
iNOS
ONOO-
Anti-leishmanial
NO